*Egypt. J. Chem.* **Vol. 64**, No. 10, pp. 5511 – 5519 (2021)

**Egyptian Journal of Chemistry**

**http://ejchem.journals.ekb.eg/**

# Adsorption of Tetracycline Antibiotic from Aqueous Solutions using Natural Iraqi Bentonite

**Shahad Mahmood Khalaf,[a] Saddam Mohammed Al-Mahmoud,[a,*]**

[a]*Department of Chemistry, College of Education for Women, Tikrit University, Tikrit, Iraq*

**Abstract**

Natural Iraqi bentonite was employed in this study as inexpensive adsorbent for the removal of Tetracycline hydrochloride antibiotic from aqueous solutions. The removal of about 90% of the Tetracycline was achieved under the optimum adsorption conditions of 2 *h* equilibrium time, 0.2 *g* bentonite dose, 20 *mg/L* initial Tetracycline concentration, and at a pH between 6 and 7. The thermodynamic investigation was carried out at various temperatures ranging between 20-40 °C. The resulted thermodynamic parameters emphasize a decrease of the randomness, an exothermic, and a spontaneous nature of the adsorption process arising from the negative values of the entropy change, the enthalpy change, and the Gibbs free energy change, respectively. The kinetic studies showed that the pseudo-second order model could fulfill a better fit of the experimental data, and more than one process would influenced the diffusion of tetracycline from the solution into the bentonite. The Isotherm studies reveals that Langmuir model provided a best fit to the isotherm curve, with a maximum adsorption capacity of 23.69 $mg\ g^{-1}$. The results suggest that Natural Iraqi bentonite can be used as a cost-effective adsorbent for the removal of Tetracycline hydrochloride from aqueous mediums.

Keywords: Antibiotics; Tetracycline; Bentonite; Adsorption.

## 1. Introduction

Water pollution remains a critical global threat [1]. The presence of chemical pollutants in wastewater has gained increasing importance in recent years [2]. These chemical pollutants such as pharmaceuticals, surfactants, dyes, and heavy metals can easily permeate to the environment and cause a potential risk to the organisms [3].

Recently, residual antibiotics have been discovered in the surface and ground water all over the world [4, 5]. Due to their efficiency to treat diseases resulted from infection; antibiotics are widely used in large quantities to control diseases that influence the organisms [6]. Tetracycline hydrochloride (TCN) is one of the most important pharmaceutical antibiotics used in the treatment of many infections caused by various types of infectious bacteria [7, 8]. It has been commonly applied to treat animal diseases, including adding it to animal feed to enhance their growth [3]. Because of its high solubility in water, it was found that TCN through the use of organic fertilizers for plants, can reach the soil and also the aquatic ecosystem [9]. A large part of these antibiotics is not used in the metabolism process as it passes through the body of the organisms and is throw to the environment causing a contamination of water resources [10]. Although the concentrations of antibiotics in ground and surface waters are relatively low [11], their continued existence threatens environmental life, and their impacts should not be neglected [12]. Therefore, it is substantial to remove antibiotic remains from their main sources before discharging them into the aquatic environment.

Several techniques have been widely used for removal of various antibiotics from aqueous solutions including Ozonation [13, 14], Advanced oxidation processes [15], Photo-catalytic degradation [16–18], Coagulation [19, 20], and Adsorption [21–23]. However, it possess a numerous obstacles including low efficiency, complicated operation, and toxic by-

*Corresponding author e-mail: s_almahmoud@tu.edu.iq
Receive Date: 16 May 2021, Revise Date: 24 May 2021, Accept Date: 26 May 2021
DOI: 10.21608/EJCHEM.2021.76358.3734

product generation [1]. Among these methods, adsorption is promising for water purification due to its simplicity in fabrication, inexpensive, high performance, and absence of toxic intermediates [23–25]. Many adsorbents have been used to remove water pollutants such as activated carbon [26–28], metal oxides [29, 30], clays [31], and agricultural wastes [32,33]. However, the low economic cost of natural adsorbents has led researchers to focus on its widely utilization in water remediation [4].

Clays are natural adsorbents exists in high abundance in the nature [34]. Clays known for its ability to intercalate pharmaceuticals into the layered structure has stimulated its utilization in drug delivery [35]. Among the used clays, Bentonite is one of the most available natural mineral that widely have been utilized in waste and toxins disposal from aqueous medium [36]. Bentonite have been one of the significant raw material used in various applications [37]. Its applicability in environmental and industrial applications is mainly due to its availability, and non-toxicity, low cost, porous structure, large surface area, higher thermal and chemical stability, and high cation exchangeability [38].

The objective of this project is to evaluate the ability of local Iraqi bentonite on the deportation of Tetracycline hydrochloride antibiotic from aqueous solutions, and to assess the extreme effective conditions that influence the adsorption operation.

## 2. Materials and Methods

### *2.1. Materials*

Tetracycline hydrochloride (TCN) with was provided from the state company for drugs industry and medical appliances in Samarra (Iraq), and it was used as received without any further purification. The chemical structures of TCN is displayed in Fig. 1. The clay used in this work is a natural Iraqi bentonite (IBT) that was collected from the region of Diyala (eastern of Iraq). It was first washed several times with deionized water and then washed with ethanol at 50 ºC for 1 *h*. in order to eliminate any impurities. The sample was then dried in the oven at 105 ºC for 2 *h*. and sieved using molecular sieves (Retsch, Germany) to obtain small particles with a size less than 100 µm. The field emission scanning electron microscopy (FESEM) was employed to characterized the surface morphology of the natural Iraqi bentonite.

### *2.2. Adsorption Experiments*

A stock solution of TCN with a concentration of

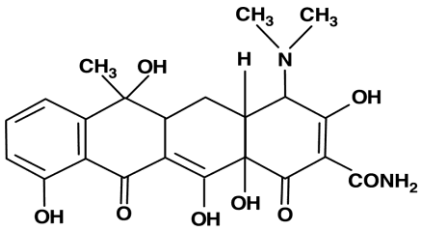


**Fig. 1. The chemical structure of TCN.**

250 *mg/L* is prepared by dissolving TCN in deionized water and used it further to obtain concentrations in demand. The effects of a diverse factors including pH (3-10), bentonite dosage (0.01-0.3 *g*), contact time (10-180 min), initial TCN concentration (20-100 mg/L), and temperature (20-40 °C) on the adsorption of TCN on IBT are examined. The adsorption experiments were carried out in 100 ml conical flask with 25 ml of TCN solution. To get a superior agitating performance, each solution is shaken using a controlled shaking water bath (GFL, Germany) using a speed of 120 rpm. After adsorption, each solution was centrifuged at a speed of 4000 rpm for 5 min by utilizing (Gallenkamp centrifuge, England) to get the supernatant with the remained TCN concentration. The residual TCN were measured at 360 nm using UV–Visible Spectrophotometer (UVD-3000, LABOMED, INC). The amount of TCN adsorbed on the IBT surface was then acquired from the concentration difference. Moreover, an acidic solution of 0.1 M of hydrochloric acid and an alkaline solution of 0.1 M of sodium hydroxide were employed to adjust the pH of the TCN solutions to the appropriate values.

The adsorption efficiency (% Adsorption), and the amount of TCN adsorbed per gram of IBT $q_t$ (*mg/g*) were determined using the following equations, respectively:

$$\%\, Adsorption = \frac{(C_0 - C_e)}{C_0} \times 100 \qquad (1)$$

$$q_t = \frac{(C_0 - C_t)V}{m} \qquad (2)$$

Where, $C_o$ is the initial TCN concentration (*mg/L*), $C_e$ and $C_t$ are the TCN concentration (*mg/L*) at equilibrium and at time (*t*), respectively, *V* is the volume of the TCN solution (*L*), and *m* is the mass of the IBT clay (*g*).

The main thermodynamic parameters for the TCN adsorption onto IBT were estimated from the following equations:

$$\Delta G = -\, RT\, \ln K_e \qquad (3)$$

$$\ln K_e = \frac{\Delta S}{R} - \frac{\Delta H}{RT} \qquad (4)$$

Where, $\Delta H$ is the enthalpy change ($J\ mol^{-1}$), $\Delta S$ is the entropy change ($J\ mol^{-1}\ K^{-1}$), $\Delta G$ is the free energy change ($J\ mol^{-1}$), $R$ is the gas constant (8.314 J $mol^{-1}\ K^{-1}$), $T$ is the absolute temperature ($K$), and $K_e$ is the equilibrium constant that can be obtained from:

$$K_e = \frac{C_0 - C_e}{C_e} \quad (5)$$

The kinetic studies of the TCN adsorption onto IBT were estimated for the experimental data by employing four kinetic models, the pseudo-first order model [39], pseudo-second order model [40], Intraparticle diffusion model [41], and Elovich model [42], whose linearized equations are given in Eqs. (6) – (9), respectively:

$$\ln(q_e - q_t) = \ln q_e - k_1\, t \quad (6)$$

$$\frac{t}{q_t} = \left(\frac{1}{k_2\, q_e^2}\right) + \left(\frac{1}{q_e}\right) t \quad (7)$$

$$q_t = k_{int}\, t^{1/2} + C \quad (8)$$

$$q_t = \left(\frac{1}{\beta}\right) \ln \alpha\beta + \left(\frac{1}{\beta}\right) \ln t \quad (9)$$

Where $q_e$ and $q_t$ are the adsorption capacities ($mg/g$) at equilibrium and at time ($t$), respectively. $k_1$ is the pseudo-first order rate constant ($min^{-1}$), $k_2$ is the pseudo-second order rate constant ($g.\ mg^{-1}.\ min^{-1}$). $k_{int}$ is the intraparticle diffusion constant (mg. $g^{-1}$. $min^{-1/2}$), and C is the intercept, which is proportional to the thickness of the boundary layer thickness. $\alpha$ ($mg\ g^{-1}\ min^{-1}$) and $\beta$ ($g\ mg^{-1}$) are the Elovich's constant that give the information about the initial rate of the removal and extent of surface coverage for chemisorption, respectively.

The isothermal studies was performed using Freundlich and Langmuir isotherm models, whose linearized form can be given in equation (10) and (11) respectively:

$$\ln q_e = \ln K_F + \frac{1}{n} \ln C_e \quad (10)$$

$$\frac{1}{q_e} = \frac{1}{q_m} + \left(\frac{1}{q_m K_L}\right) \frac{1}{C_e} \quad (11)$$

Where $K_F$ and $n$ are the Freundlich constants linked to the adsorption capacity and adsorption intensity, respectively. The value of $n$ can provide a denotation of the compatibility of adsorption system. If $n < 1$, this reveals that the process is chemisorption; while if $n > 1$adsorption process is physical [1]. $q_m$ is an essential parameter denotes the superior adsorption capacity ($mg/g$), and $K_L$ is the Langmuir affinity constant correspond to the required energy for the adsorption ($L/mg$).

## 3. Results and Discussion

### *3.1. Characterization of IBT*

The surface morphology of the natural Iraqi bentonite used in this work was characterized by employing the field emission scanning electron microscopy (FESEM). The high resolution FESEM image for the surface morphology of IBT is shown in Fig. 2. It can be clearly observed irregular shapes with various particle sizes. In addition, an unsmooth and rough surface with a small particles less than 100 nm sizes can supply more surface area to allocate superior contact between the IBT adsorbent surface and the antibiotic molecules.

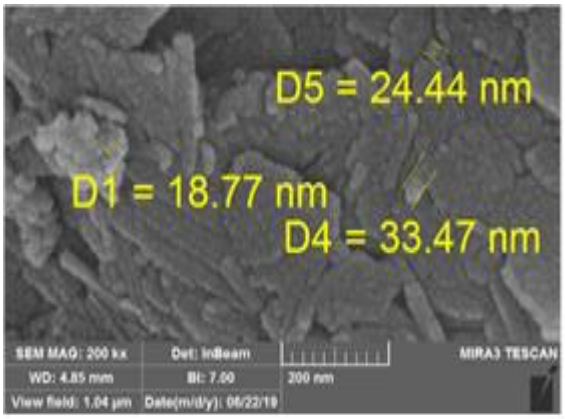


Fig. 2. FESEM image of natural Iraqi bentonite.

### *3.2. Effect of pH on the adsorption of TCN onto IBT*

The pH of the medium is a substantial parameter affecting the TCN removal on the bentonite surface. The pH impact on TCN removal was investigated between 3-10 using the initial TCN concentration of 20 *mg/L*, bentonite dose of 0.2 *g*, equilibrium time of 120 min., and at 20 °C. Tetracycline hydrochloride is recognized to present in the solution with different forms, and each form relies on the pH values. Under acidic conditions it exist as $H_4TCN^+$, and it present as $H_2TCN^-$ at the basic conditions, while close to neutral the dominant form is $H_3TCN$ [8]. The variation of the pH on TCN uptake onto IBT surface are presented in Fig. 3. It can be clearly seen a low TCN adsorption under acidic conditions. At lower pH values, hydrogen ions $H^+$ would adsorbed on the IBT surface, causing the clay to have more positively charged surface. Thus, the electrostatic repulsion of

the $H_4TCN^+$ with the clay surface can lower the adsorption efficiency [36]. The opposite is true under basic conditions, where $H^+$ are separate from the IBT surface, causing the clay surface to become more negative. Thus, the electrostatic repulsion of the $H_2TCN^-$ with the negatively charged IBT surface can lower the uptake level of the antibiotic.

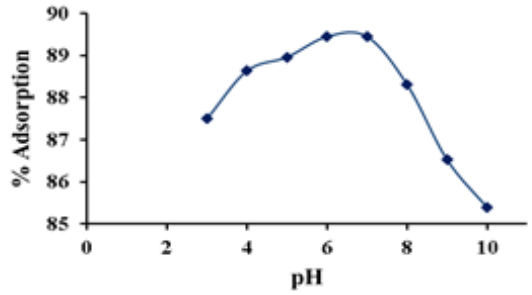


**Fig. 3. Effect of the pH on the adsorption of TCN onto IBT.**

In addition, the superior adsorption efficiency can be attained at a pH between 6 and 7 that is nearly to the natural pH of the TCN solution used in this work, which is about 6.5. At this pH the antibiotic present as $H_3TCN$ where the inhibitory electrostatic repulsion were decreased. This indicates that adsorption of TCN was disfavored in highly acidic or basic extent; therefore all solutions were tested at the pH of 6.5 that considered the normal value of TCN in the aqueous medium.

### *3.3. Effect of IBT dose on the adsorption of TCN*

The variation of the IBT amount as a function of the TCN removal efficiency was studied using a normal pH solution of 6.5, 20 *mg/L* initial TCN concentration of, 120 min equilibrium time, and at 20 °C. Fig. 4 shows the effect of IBT clay on the adsorption of TCN from aqueous solutions. A low adsortion efficiency of about 35% can be seen when small dose of 0.01 g of IBT was utilized. Also, a gradual rise of the removal efficiency of TCN was observed as the clay amount increased to reach its highest value of about 90% using 0.2 *g* of IBT. The availability of the active adsorption sites on the adsorbent surface play a crucial role in explaining this result [33]. So that, it is more probably that employing a small amount of the clay can take off a small amount of TCN molecules. Increasing the clay dosage can provide more adsorption sites to remove additional TCN molecules, which can result in a greater increase in the removal efficiency. Further increase in the clay dose does not show any significant change of the adsorption efficiency, which could contribute to achieving the equilibrium state.

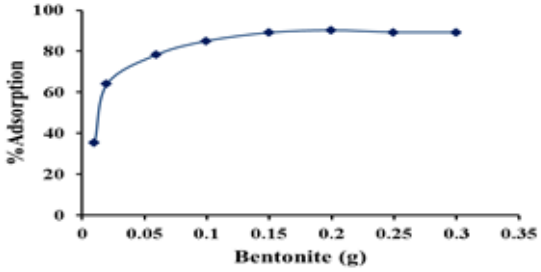


**Fig. 4. Effect of the IBT dose on the adsorption of TCN.**

### *3.4. Effect of contact time on the adsorption of TCN onto IBT*

The influence of contact time on the removal of TCN on bentonite clay was investegated with various contact times ranged from 10-180 min. using a normal pH solution of 6.5, TCN initial concentration of 20 *mg/L*, bentonite dose of 0.2 *g*, and at a temperature of 20 °C. The adsorption efficiency of 60% was observed after only 10 min, as shown in Fig. 5, indicating a good affinity between TCN particles and IBT surface that is refer to the presence of a considerable number of unoccupied adsorption sites on the IBT surfaces. In addition, as the contact time increases, the adsorption of TCN on the IBT surface increases and the uptake rate becomes slower consequent to the decline in the available Adsorption sites, and to the slow diffusion within the pores of the clay particles [9].

Moreover, After 120 minutes the removal process stabilized and remains constant. This means that no additional adsorption could occur after this time, which indicate that the equilibrium has accomplished in 120 min. After attaining equilibrium, the remaining sites are hard to occupy due to the resistance between TCN particles on the IBT surface and the incoming TCN particles [32].

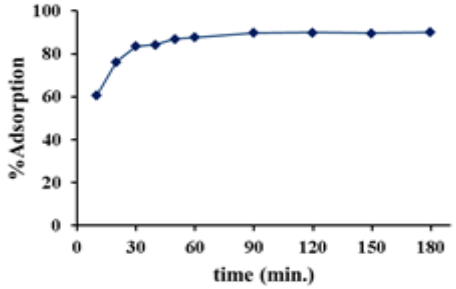


**Fig. 5. Effect of the contact time on the adsorption of TCN onto IBT.**

*3.5. Effect of TCN initial concentration on its adsorption onto IBT*

The effect of TCN initial concentration on the removal efficiency was tested using various concentrations ranging from 20-100 *mg/L*, normal pH solution of 6.5, equilibrium time of 120 min., bentonite dose of 0.2 *g*, and at a temperature of 20 °C. The results are presented in Fig. 6, which shows an adsorption efficiency of about 85% at a concentration of 20 *mg/L*. A progressive decline in the uptake level was noticed as the antibiotic concentration increase. This indicates that the residual antibiotic concentration will be higher for higher initial antibiotic concentrations, which can be associated with the decline in the relative number of the free adsorption sites that required to take off the antibiotic molecules [43, 44].

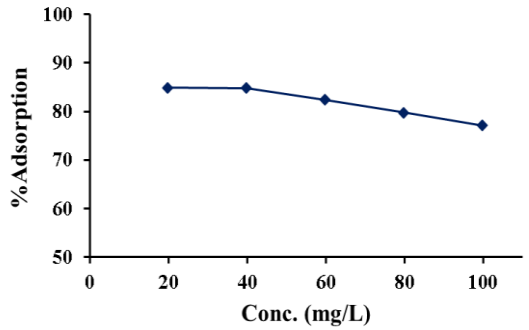


**Fig. 6. Effect of the TCN initial concentration on the adsorption of TCN onto IBT.**

*3.6. Effect of Temperature on the adsorption of TCN onto IBT and Thermodynamic Study.*

The effect of temperature on the removal of TCN by IBT was investigated using various temperatures ranging between 293-313 °C, normal pH solution of 6.5, initial TCN concentration of 20 *mg/L*, bentonite dose of 0.2 *g*, and an equilibrium time of 120 min. Fig. 7 displays the adsorption efficiency as a function of temperature. A perfect adsorption efficiency of about 90% was noticed at a lowest temperature, and as the temperature increases, the uptake level decreases. Elevating the temperature can break the attraction forces between adsorbate and adsorbent [30], which may promote the ability of TCN molecules to separate from IBT particles. This suggests that removing TCN on the IBT clay is an exothermic process, and elevating the temperature would result in reducing the adsorption efficiency.

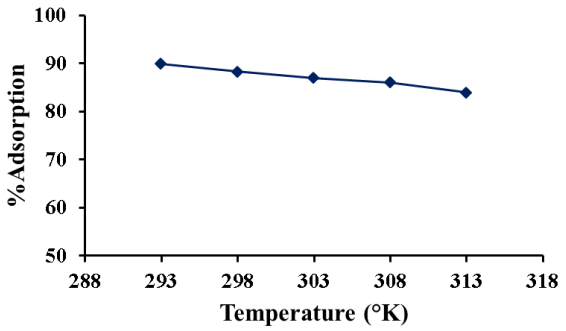


**Fig. 7. Effect of the temperature on the adsorption of TCN onto IBT.**

These experimental data at several temperatures were further analyzed to determine the thermodynamic parameters for the adsorption operation. The Gibbs free energy changes $\Delta G$ were determined from equation (3), while the enthalpy change $\Delta H$ and the entropy change $\Delta S$ were estimated using equation (4) from the slope (2344.8) and intercept (-5.8257) of the straight line of the plot between ln $K$ versus $1/T$, respectively. The resulted thermodynamic parameters are listed in Table 1.

**Table 1: Thermodynamic parameters for the TCN adsorption onto IBT surface at various temperatures.**

| $T$ (°K) | $\Delta H$ ($J\ mol^{-1}$) | $\Delta S$ ($J\ mol^{-1}\ K^{-1}$) | $\Delta G$ ($J\ mol^{-1}$) | $R^2$ |
|---|---|---|---|---|
| 293 | -19494.7 | -48.4349 | -5334.92 | 0.9888 |
| 298 | | | -5010.35 | |
| 303 | | | -4791.68 | |
| 308 | | | -4656.73 | |
| 313 | | | -4301.37 | |

The calculated thermodynamic parameters suggest a decrease in the randomness during the interaction of TCN with IBT particles that refers to the negative value of $\Delta S$. Also, an exothermic behavior of the removal process attributes to the negative value of $\Delta H$ that is in agreement with what was mentioned earlier, which shows that the removal of TCN on IBT surface decreased with elevated temperature (see Fig.

7). Moreover, a spontaneous nature of the removal process revealed from the negative values of $\Delta G$, and elevating the temperature leads to an increase in the $\Delta G$ values, which indicates that the uptake of TCN on IBT is less preferable with elevated temperature.

### *3.7. Kinetic studies*

The kinetic studies provide beneficial insights into the description of the uptake rate and therefore modelling the removal process. The pseudo-first order Eq. (6) and the pseudo-second order Eq. (7) rate equations are widely applied for modeling the experimental data acquired from adsorption process [23]. These two models were applied in this project to assess the adsorption data of TCN removal onto IBT, and the results are presented in Table 2.

**Table 2: Kinetic parameters for the TCN adsorption onto IBT surface.**

| Kinetic model | Parameter | value |
|---|---|---|
| | $q_e$ exp. (mg. g$^{-1}$) | 2.248 |
| Pseudo-first order | $q_e$ cal. (mg. g$^{-1}$) | 1.336 |
| | $k_1$ (min$^{-1}$) | 0.139 |
| | $R^2$ | 0.968 |
| Pseudo-second order | $q_e$ cal. (mg. g$^{-1}$) | 2.306 |
| | $k_2$ (g. mg$^{-1}$. min$^{-1}$) | 0.117 |
| | $R^2$ | 0.999 |
| Elovich | $\alpha$ (mg g$^{-1}$. min$^{-1}$) | 51.306 |
| | $\beta$(g mg$^{-1}$) | 4.496 |
| | $R^2$ | 0.789 |
| Intraparticle diffusion | $k_{int\,(1)}$ (mg. g$^{-1}$. min$^{-1/2}$) | 0.251 |
| | $k_{int\,(2)}$ (mg. g$^{-1}$. min$^{-1/2}$) | 0.040 |
| | $k_{int\,(3)}$ (mg. g$^{-1}$. min$^{-1/2}$) | 0.001 |
| | $R^2_{(1)}$ | 0.982 |
| | $R^2_{(2)}$ | 0.943 |
| | $R^2_{(3)}$ | 0.144 |

Based on the correlation coefficient $R^2$ values, it can derive that a best fitted kinetic model is with the pseudo-second order rate equation. It also clarifies that the calculated adsorption capacity ($q_e$ cal.) resulted from applying pseudo-second order is much adjacent to the experimental value ($q_e$ exp.). This finding emphasizes that the TCN adsorption on IBT surface followed the pseudo-second order model, which endorsed the chemisorption nature of the process that comprises sharing or exchanging of electrons between TCN particles and IBT surface. Moreover, the Elovich model is useful for describing the heterogeneous surfaces. The smaller value of $R^2$ denote that Elovich model is inconvenience for evaluating the adsorption data that confirms that the IBT surface is a homogenous surface.

Further analysis of the adsorption data were employed using intraparticle diffusion model Eq. (8), to explore the rate dominant step in the TCN removal onto IBT. The intraparticle diffusion plot of the TCN amount versus the square root of time is illustrated in Fig. 8. It can be clearly seen a collection of three steps that can be observed usually using this model [45, 46]. The first step was related to the mass transfer across the boundary layer surrounding the external adsorbent surface. The intraparticle diffusion within the internal framework of the adsorbent particle is the intermediate step. Finally, an adsorption equilibrium starts take place, where the intraparticle diffusion become slower attributed to the considerably low adsorbate concentrations remains in the solution. In addition, if the intraparticle diffusion is the rate-controlling step in the adsorption process, then it should give a straight line passing within the origin [47]. The non-linearity of the plot over the whole time extent was clearly observed, and it does not pass over the origin, which reveals that the adsorption of TCN onto IBT is influenced by more than one process and the intraparticle diffusion is not the controlling step in the removal process.

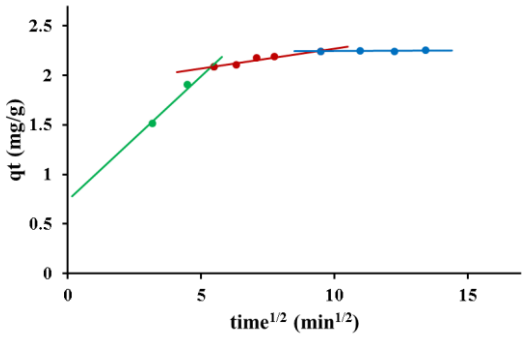


**Fig. 8. Intraparticle diffusion plot for the TCN adsorption onto IBT.**

*3.8. Isothermal studies*

The adsorption isotherm describes the mechanism engaged in the adsorption operation. Freundlich and Langmuir isotherms consider as the most ordinarily utilized isotherms in the removal studies. Freundlich isotherm describes the heterogeneity of the adsorbent surface and assumes a multilayer surface coverage [48], while Langmuir isotherm assumes a monolayer adsorption where a homogenous distribution of the adsorption energy through the whole coverage of the adsorbent surface [49].

The experimental equilibrium data for the influence of initial TCN concentration on its adsorption onto IBT were further analyzed to fit with Freundlich (Eq. (10)) and Langmuir (Eq. (11)) isotherm models. The linear plots of the employed models are presented in Fig. 9, and the isotherm parameters are summed up in table 3.

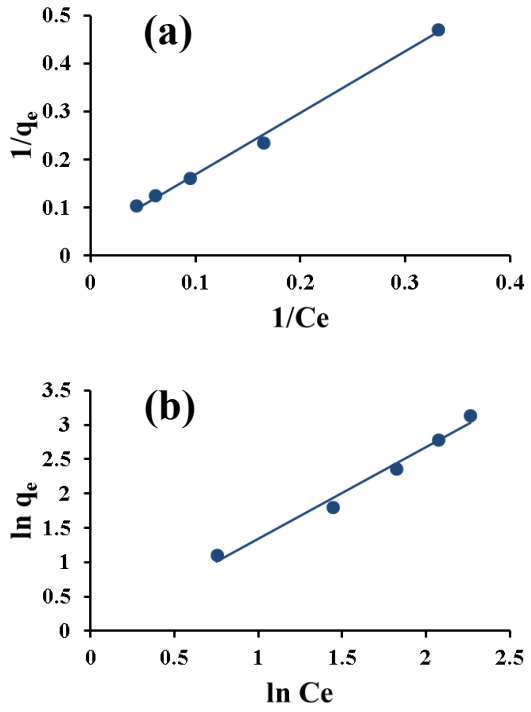


**Fig. 9. Langmuir (a), Freundlich (b) adsorption isotherm plots for the adsorption of TCN onto IBT.**

The dimensionless constant separation factor $R_L$ considers an essential characteristic of Langmuir model that can be obtained by:

$$R_L = \frac{1}{(1 + k_L C_0)} \qquad (12)$$

$R_L$ magnitude can be used to elucidates the possibility of the adsorption system being unfavorable if ($R_L > 1$), linear if ($R_L = 1$), favorable if ($0 < R_L < 1$), or irreversible if ($R_L = 0$). The $R_L$ values were obtained to be in the extent of 0.231–0.857, while $n$ value was obtained to be less than 10, indicating the favorability of the removal process. In addition, a linear pattern was observed for both isotherms, with a better fit of the data with Langmuir isotherm as indicated from their $R^2$ values, which proposes that the TCN removal onto IBT applied to Langmuir isotherm. Moreover, The maximum adsorption capacity of IBT was found to be 23.69 *mg* $g^{-1}$, which is greater than that of agricultural waste ($q_m$ = 15.52 *mg* $g^{-1}$) [8].

**Table 3: Isothermal parameters for the TCN adsorption onto IBT surface**

| Isothermal model | Parameter | value |
|---|---|---|
| Freundlich | $K_F$ (mg. $g^{-1}$) | 1.010 |
| | $n$ | 0.75 |
| | $R^2$ | 0.983 |
| Langmuir | $q_m$ (mg. $g^{-1}$) | 23.69 |
| | $k_L$ (L $mg^{-1}$) | 0.033 |
| | $R^2$ | 0.995 |
| | $R_L$ | 0.231 - 0.857 |

## 4. Conclusions

In this work, the ability of Natural Iraqi bentonite as effective and low-cost adsorebent material to remove Tetracycline hydrochloride from aqueous solutions was examined. The optimal adsorption conditions obtained to be 0.2 *g* clay dose, 2 h contact time, 20 *mg/L* initial antibiotic concentration, and pH between 6 and 7. The temperature would influence the removal process, and rising the temperature would decrease the uptake level. A decline in the randomness, an exothermic, and spontaneous nature of the adsorption process were indicated from the negative amounts of the thermodynamic operators. A better fit of the data was obtained by applying Langmuir isotherm with a maximum adsorption capacity for the bentonite of 23.69 *mg* $g^{-1}$. The pseudo second-order model well described the adsorption kinetic, and the intraparticle diffusion does not solely the rate-controlling step in the removal process. The existing work displays that Natural Iraqi bentonite can be an efficient adsorbent for removing tetracycline hydrochloride from aqueous solutions.

## Acknowledgments

This research was supported by Tikrit University, Ministry of Higher Education and Scientific research, Iraq.

## References

[1] Paunovic O., Pap S., Maletic S., Taggart M.A., Boskovic N., Turk Sekulic M., Ionisable emerging pharmaceutical adsorption onto microwave functionalised biochar derived from novel lignocellulosic waste biomass, *J. Colloid Interface Sci.*, **547**, 350–360 (2019).

[2] Başaran Dindaş G., Çalışkan Y., Çelebi E.E., Tekbaş M., Bektaş N., Yatmaz H.C., Treatment of pharmaceutical wastewater by combination of electrocoagulation, electro-fenton and photocatalytic oxidation processes, *J. Environ. Chem. Eng.*, **8**, 103777 (2020).

[3] Yazidi A., Atrous M., Edi F., Ismadji S., Erto A., Bonilla-petriciolet A., Luiz G., Ben A., Adsorption of amoxicillin and tetracycline on activated carbon prepared from durian shell in single and binary systems : Experimental study and modeling analysis, *Chem. Eng. J.*, **379**, 122320 (2020).

[4] Bao X., Qiang Z., Chang J.H., Ben W., Qu J., Synthesis of carbon-coated magnetic nanocomposite (Fe3O4 at C) and its application for sulfonamide antibiotics removal from water, *J. Environ. Sci.*, **26**, 962–969 (2014).

[5] Peng X., Hu F., Dai H., Xiong Q., Xu C., Study of the adsorption mechanisms of ciprofloxacin antibiotics onto graphitic ordered mesoporous carbons, *J. Taiwan Inst. Chem. Eng.*, **65,** 472–481 (2016).

[6] Khraisheh M., Kim J., Campos L., Al-Muhtaseb A.H., Al-Hawari A., Al Ghouti M., Walker G.M., Removal of pharmaceutical and personal care products (PPCPs) pollutants from water by novel TiO2-Coconut Shell Powder (TCNSP) composite, *J. Ind. Eng. Chem.*, **20**, 979–987 (2014).

[7] Lin Y., Xu S., Jia L., Fast and highly efficient tetracyclines removal from environmental waters by graphene oxide functionalized magnetic particles, *Chem. Eng. J.*, **225**, 679–685 (2013).

[8] Hoslett J., Ghazal H., Katsou E., Jouhara H., The removal of tetracycline from water using biochar produced from agricultural discarded material, *Sci. Total Environ.*, **751,** 141755 (2021).

[9] Sayğili H., Güzel F., Effective removal of tetracycline from aqueous solution using activated carbon prepared from tomato (Lycopersicon esculentum Mill.) industrial processing waste, *Ecotoxicol. Environ. Saf.*, **131**, 22–29 (2016).

[10] Bangari R.S., Sinha N., Adsorption of tetracycline , ofloxacin and cephalexin antibiotics on boron nitride nanosheets from aqueous solution, *J. Mol. Liq.*, **293**, 111376 (2019).

[11] Vona A., Garcia-ivars J., Picó Y., Comparison of different removal techniques for selected pharmaceuticals, *J. Water Process Eng.*, **5**, 48–57 (2015).

[12] Quesada H.B., Baptista A.T.A., Cusioli L.F., Seibert D., de Oliveira Bezerra C., Bergamasco R., Surface water pollution by pharmaceuticals and an alternative of removal by low-cost adsorbents: A review, *Chemosphere*, **222**, 766–780 (2019).

[13] Feng M., Yan L., Zhang X., Sun P., Yang S., Wang L., Wang Z., Fast removal of the antibiotic fl umequine from aqueous solution by ozonation : In fl uencing factors , reaction pathways , and toxicity evaluation, *Sci. Total Environ.*, **541**, 167–175 (2016).

[14] Gomes J., Costa R., Quinta-ferreira R.M., Martins R.C., Application of ozonation for pharmaceuticals and personal care products removal from water, *Sci. Total Environ.*, **586**, 265–283 (2017).

[15] Klavarioti M., Mantzavinos D., Kassinos D., Removal of residual pharmaceuticals from aqueous systems by advanced oxidation processes, *Environ. Int.*, **35**, 402–417 (2009).

[16] Hapeshi E., Achilleos A., Vasquez M.I., Michael C., Xekoukoulotakis N.P., Mantzavinos D., Kassinos D., Drugs degrading photocatalytically : Kinetics and mechanisms of ofloxacin and atenolol removal on titania suspensions, *Water Res.*, **44**, 1737–1746 (2010).

[17] Hao R., Xiao X., Zuo X., Nan J., Zhang W., Efficient adsorption and visible-light photocatalytic degradation of tetracycline hydrochloride using mesoporous BiOI microspheres, *J. Hazard. Mater.*, **209–210**, 137–145 (2012).

[18] Niu J., Xie Y., Luo H., Wang Q., Zhang Y., Wang Y., Cobalt oxide loaded graphitic carbon nitride as adsorptive photocatalyst for tetracycline removal from aqueous solution, *Chemosphere*, **218**, 169–178 (2018).

[19] Yang W., Wu Y., Zhang L., Jiang J., Feng L., Removal of five selected pharmaceuticals by coagulation in the presence of dissolved humic acids and kaolin, *Desalin. Water Treat.*, **54,** 1134–1140 (2015).

[20] Sheng C., Nnanna A.G.A., Liu Y., Vargo J.D., Removal of Trace Pharmaceuticals from Water using coagulation and powdered activated carbon as pretreatment to ultra fi ltration membrane system, *Sci. Total Environ.*, **550**, 1075–1083 (2016).

[21] Darweesh T.M., Ahmed M.J., Adsorption of ciprofloxacin and norfloxacin from aqueous solution onto granular activated carbon in fixed bed column, *Ecotoxicol. Environ. Saf.*, **138,** 139–145 (2017).

[22] Madimetja J., Nomngongo P.N., Effective adsorptive removal of amoxicillin from aqueous solutions and wastewater samples using zinc oxide coated carbon nano fiber composite, *Emerg. Contam.*, **5**, 143–149 (2019).

[23] Mohammed A.A., Al-Musawi T.J., Kareem S.L., Zarrabi M., Al-maabreh A.M., Simultaneous

adsorption of tetracycline , amoxicillin , and ciprofloxacin by pistachio shell powder coated with zinc oxide nanoparticles, *Arab. J. Chem.*, **13**, 4629–4643 (2020).

[24] Kyzas G.Z., Fu J., Lazaridis N.K., Bikiaris D.N., Matis K.A., New approaches on the removal of pharmaceuticals from wastewaters with adsorbent materials, *J. Mol. Liq.*, **209,** 87–93 (2015).

[25] Dhiman N., Sharma N., Removal of pharmaceutical drugs from binary mixtures by use of ZnO nanoparticles: (Competitive adsorption of drugs), *Environ. Technol. Innov.*, **15**, 100392 (2019).

[26] Torres-Pérez J., Gérente C., Andrès Y., Sustainable activated carbons from agricultural residues dedicated to antibiotic removal by adsorption, *Chinese J. Chem. Eng.*, **20,** 524–529 (2012).

[27] Chayid M.A., Ahmed M.J., Amoxicillin adsorption on microwave prepared activated carbon from Arundo donax Linn: Isotherms, kinetics, and thermodynamics studies, *J. Environ. Chem. Eng.*, **3,** 1592–1601 (2015).

[28] Acosta R., Fierro V., Martinez de Yuso A., Nabarlatz D., Celzard A., Tetracycline adsorption onto activated carbons produced by KOH activation of tyre pyrolysis char, *Chemosphere*., **149**, 168–176 (2016).

[29] Dhiman N., Sharma N., Removal of ciprofloxacin hydrochloride from aqueous solution using vertical bed and sequential bed columns, *J. Environ. Chem. Eng.*, **6**, 4391–4398 (2018).

[30] Al-Mahmoud S.M., Adsorption of Some Alephatic Dicarboxylic Acids on Zinc Oxide: A kinetic and Thermodynamic Study, *Baghdad Sci. J.*, **16,** 892–897 (2019).

[31] Tahir S.S., Rauf N., Removal of a cationic dye from aqueous solutions by adsorption onto bentonite clay, *Chemosphere*, **63**, 1842–1848 (2006).

[32] Al-Mahmoud S.M., Kinetic, Isothermal and Thermodynamic Investigations for the Use of Pumpkin Seed Husks as low-Cost Biosorbent of Solochrome Cyanine R from Aqueous Solutions, *Egypt. J. Chem.*, **63**, 2947–2957 (2020).

[33] Al-Mahmoud S.M., Kinetic and Thermodynamic Studies for the Efficient Removal of Methylene Blue Using Hordeum Murinum as a New Biosorbent, *Egypt. J. Chem.*, **63**, 3381–3390 (2020).

[34] Ahmadi S., Adaobi C., Adsorptive removal of phenol and aniline by modified bentonite : adsorption isotherm and kinetics study, *Appl. Water Sci.*, **8,** 1–8 (2018).

[35] Arya V., Philip L., Adsorption of pharmaceuticals in water using Fe3O4 coated polymer clay composite, *Microporous Mesoporous Mater.*, **232**, 273–280 (2016).

[36] Radwan N.R.E., Hagar M., Chaieb K., Adsorption of crystal violet dye on modified bentonites, *Asian J. Chem.*, **28**, 1643–1647 (2016).

.

[37] El Miz M., Akichoh H., Berraaouan D., Salhi S., Tahani A., Chemical and Physical Characterization of Moroccan Bentonite Taken from Nador ( North of Morocco ), *Am. J. Chem.*, **7**, 105–112 (2017).

[38] Dardir F.M., Mohamed A.S., Abukhadra M.R., Ahmed E.A., Soliman M.F., Cosmetic and pharmaceutical qualifications of Egyptian bentonite and its suitability as drug carrier for Praziquantel drug, *Eur. J. Pharm. Sci.*, **115**, 320–329 (2018).

[39] Lagergren S., About the Theory of So-Called Adsorption of Soluble Substances, K. Sven. *Vetenskapsakademiens Handl.*, **24**, 1–39 (1898).

[40] Ho Y.S., McKay G., A Comparison of chemisorption kinetic models applied to pollutant removal on various sorbents, *Process Saf. Environ. Prot.*, **76**, 332–340 (1998).

[41] Weber W.J., Morris J.C., Kinetics of Adsorption on Carbon from Solution, *J. Sanit. Eng. Div.*, **89,** 31–60 (1963).

[42] Zeldowitsch J., über Den Mechanismus der Katalytischen Oxidation Von CO a MnO2, *Acta Physicochim. URSS.*, **1,** 364–449 (1934).

[43] Pal A., Pan S., Saha S., Synergistically improved adsorption of anionic surfactant and crystal violet on chitosan hydrogel beads, *Chem. Eng. J.*, **217**, 426–434 (2013).

[44] Sulyman M., Kucinska-lipka J., Sienkiewicz M., Gierak A., Development , characterization and evaluation of composite adsorbent for the adsorption of crystal violet from aqueous solution : Isotherm , kinetics , and thermodynamic studies, *Arab. J. Chem.*, **14,** 103115 (2021).

[45] Daifullah A.A.M., Yakout S.M., Elreefy S.A., Adsorption of fluoride in aqueous solutions using KMnO 4 -modified activated carbon derived from steam pyrolysis of rice straw, *J. Hazard. Mater.*, **147**, 633–643 (2007).

[46] Cheung W.H., Szeto Y.S., Mckay G., Intraparticle diffusion processes during acid dye adsorption onto chitosan, *Bioresour. Technol.*, **98**, 2897–2904 (2007).

[47] Hameed B.H., Mahmoud D.K., Ahmad A.L., Sorption of basic dye from aqueous solution by pomelo (Citrus grandis) peel in a batch system, *Colloids Surfaces A Physicochem. Eng. Asp.*, **316**, 78–84 (2008).

[48] Freundlich H.M., Adsorption in Solution, *Zeitschrift Für Phys. Chemie.*, **57**, 385–490 (1906).

[49] Langmuir I., The adsorption of gases on plane surfaces of glass, mica and platinum, *J. Am. Chem. Soc.*, **40,** 1361–1403 (1918).